

# Effects of light scalar mesons in $\eta \rightarrow 3\pi$ decay

Abdou Abdel-Rehim<sup>a \*</sup>, Deirdre Black<sup>b †</sup>, Amir H. Fariborz<sup>c ‡</sup>, and Joseph Schechter<sup>a §</sup>

<sup>a</sup> *Department of Physics, Syracuse University, Syracuse, NY 13244-1130, USA,*

<sup>b</sup> *Jefferson Lab, 12000 Jefferson Ave., Newport News, VA 23606, USA, and*

<sup>c</sup> *Department of Mathematics/Science, State University of New York Institute of Technology, Utica, NY 13504-3050, USA.*

(Dated: October 25, 2018)

We study the role of a possible nonet of light scalar mesons in the still interesting  $\eta \rightarrow 3\pi$  decay process, with the primary motivation of learning more about the scalars themselves. The framework is a conventional non-linear chiral Lagrangian of pseudoscalars and vectors, extended to include the scalars. The parameters involving the scalars were previously obtained to fit the s-wave  $\pi\pi$  and  $\pi K$  scatterings in the region up to about 1 GeV as well as the strong decay  $\eta' \rightarrow \eta\pi\pi$ . At first, one might expect a large enhancement from diagrams including a light  $\sigma(560)$ . However there is an amusing cancellation mechanism which prevents this from occurring. In the simplest model there is an enhancement of about 13 per cent in the  $\eta \rightarrow 3\pi$  decay rate due to the scalars. In a more complicated model which includes derivative type symmetry breakers, the cancellation is modified and the scalars contribute about 30 percent of the total decay rate (although the total is not significantly changed). The vectors do not contribute much. Our model produces a reasonable estimate for the related  $a_0(980) - f_0(980)$  mixing strength, which has been a topic of current debate. Promising directions for future work along the present line are suggested.

PACS numbers: 13.75.Lb, 11.15.Pg, 11.80.Et, 12.39.Fe

## I. INTRODUCTION

There has been a revival of interest recently [1] in the possible existence of a broad scalar meson (sigma) with a mass in the 560 MeV region and its corresponding nonet partners. A large number of workers [2]-[28] have found evidence for the sigma in models of  $\pi\pi$  scattering even though it is partially obscured by background. Generally this state is considered to be of exotic nature (more complicated than  $q\bar{q}$ ) and hence an important clue to an understanding of QCD in its low energy non-perturbative regime. Similarly, analyses of  $\pi\pi$ ,  $\pi K$  and  $\pi\eta$  scattering have provided evidence for the existence of the remaining members of a possible light scalar nonet: the  $\kappa$ , the  $a_0(980)$  and the  $f_0(980)$ . In fact, the latter two states have been well established experimentally for some time. Of course, the treatment of such strongly interacting processes is inevitably model dependent and there are a number of different opinions as to the correct approach [1]. Thus it is of great interest to see whether treatments of the role of scalars in other processes using the same models employed in the scattering processes above give consistency with experiment.

From this point of view we will study the role of possible light scalars in the interesting  $\eta \rightarrow 3\pi$  decay. Typically this process has been treated by chiral perturbation theory [29], in which the possible effects of scalars have been amalgamated into effective contact interactions among the pseudoscalars. This is probably the most effective way to study the  $\eta \rightarrow 3\pi$  decay. However, our goal here is to learn more about the scalars so it is natural to keep them rather than integrating them out. Also there is a possibility that a light scalar [like the  $\sigma(560)$ ] might give an enhancement due to closeness of its propagator to the pole [see for instance Feynman diagrams like (a) and (b) of Fig.2]. Another reason for including light scalars explicitly is to become more familiar with the isospin violating  $a_0(980) - f_0(980)$  transition which should play a role in the  $\eta \rightarrow 3\pi$  decay and has also recently been postulated [30] to provide an explanation for observations of anomalously strong  $a_0(980)$  central production and the large  $\Gamma(\phi \rightarrow f_0\gamma)/\Gamma(\phi \rightarrow a_0\gamma)$  ratio. It is important to know whether the value consistent with the eta decay determination is consistent with these proposed new effects. Doubts about whether an unreasonably large value was assumed in [30] were expressed in [31].

---

\* Email: abdou@physics.syr.edu

† Email: dblack@jlab.org

‡ Email: fariboa@sunyit.edu

§ Email: schechte@physics.syr.edu

These doubts were confirmed [32] using the work of the present paper. Still another reason for the interest in the effects of the scalars in  $\eta \rightarrow 3\pi$  is to provide an orientation for the discussion of the apparently puzzling  $\eta' \rightarrow 3\pi$  decays in which light scalar mesons can be reasonably expected to have very large effects. We will give only a preliminary discussion of this process here.

In section II we give a brief historical outline of treatments of  $\eta \rightarrow 3\pi$  decay based on chiral symmetry. A number of well known ambiguities in the analysis are briefly described.

Our calculation is based on the tree level treatment of a chiral Lagrangian containing pseudoscalars, vectors and a postulated nonet of light scalars. Since the calculation is somewhat complicated, it seems to us helpful to present the results in a series of steps. First, in section III we give the results of using a Lagrangian containing only pseudoscalars with minimal symmetry breaking terms.

To this Lagrangian we add, in section IV, the scalar mesons. It will be seen that the individual scalar diagrams are quite large but there is a lot of cancellation so that the net effect is not at all dominant. However the scalars do, as desired, increase the predicted decay rate in a noticeable way. Next, the effect of adding some derivative type symmetry breakers for the pseudoscalars is described in section V. This doesn't much change the overall rate but modifies the somewhat delicate cancellations so that the scalars end up making a larger percentage contribution than before. In low energy calculations of this sort one always may expect some contributions from the vector mesons. This is discussed in section VI where it is shown that, although there is a new type of diagram the vectors do not produce a big change in the previous results.

Section VII contains a discussion of the results and directions for further work. For the convenience of readers, material describing the chiral Lagrangian used is brought together in Appendix A. Similarly the detailed expression for the decay amplitude is given in Appendix B.

## II. HISTORICAL BACKGROUND ON THE $\eta \rightarrow 3\pi$ DECAY

The study of  $\eta \rightarrow 3\pi$  has turned out to be surprisingly complicated and correspondingly important for understanding the non-perturbative (low energy) structure of QCD. Chiral dynamics in various forms has been the basic tool. Since the process violates G-parity it was initially assumed to be of electromagnetic nature, mediated by an effective photon exchange operator proportional to the product of two electromagnetic currents. The old "current algebra" approach had previously predicted the  $K_L \rightarrow \pi^+\pi^-\pi^0$  spectrum shape [33] to be

$$1 - \frac{2E_0}{m}, \quad (1)$$

where  $m$  is the  $K_L$  mass and  $E_0$  the energy of the  $\pi^0$  in the  $K_L$  rest frame. This shape, which is in reasonable agreement with experiment, resulted from the vanishing commutator of the axial charge transforming like a  $\pi^+$  with the appropriate product of two weak currents. When Sutherland [34] repeated this type of calculation for  $\eta \rightarrow \pi^+\pi^-\pi^0$  with the product of two electromagnetic currents he found that the decay amplitude was actually zero (to this leading order). Thus the  $\eta \rightarrow 3\pi$  decay did not seem to be mediated by a virtual photon emission and reabsorption. In fact, it was found [35] that a quark scalar density operator with the  $\Delta I = 1$  property proportional to

$$\bar{u}u - \bar{d}d \quad (2)$$

would give a non-zero result for the decay rate. A more detailed treatment [36] showed that the quark density operator gave the same spectrum for  $\eta \rightarrow \pi^+\pi^-\pi^0$  as in Eq.(1) with  $m$  the  $\eta$  mass in this case. Such a result is in fairly good agreement with experiment. The scalar density interaction in Eq.(2) was recognized [37] to be the fundamental up-down quark mass difference generated by the Higgs boson in the electroweak theory.

However, the predicted rates of the  $\eta \rightarrow \pi^+\pi^-\pi^0$  and  $\eta \rightarrow 3\pi^0$  modes (both the ratios and the absolute values) did not agree well with experiment at that time. Some years later, after more precise experiments, the ratio of the rates for  $\pi^+\pi^-\pi^0$  to  $3\pi^0$  modes stabilized around the value expected from isospin invariance. On the other hand the absolute rate has only recently stabilized to a value notably larger than that predicted by theory. The theory behind the current algebra results could be economically presented in the framework of an effective chiral Lagrangian. For most low energy processes where the scheme could be expected to work, the tree level computation did produce results within 25 % or so of experiment. Thus the relatively poor prediction for  $\eta \rightarrow 3\pi$  at tree level is somewhat surprising.

An improvement was obtained by Gasser and Leutwyler [29] who carried the computation of the chiral Lagrangian amplitude to one loop level. Since the non-linear chiral Lagrangian is non-renormalizable, this required the addition of new counterterms. Their finite parts were new parameters which could be mostly determined from other processes. They obtained the result  $\Gamma(\eta \rightarrow \pi^+\pi^-\pi^0) = 160 \pm 50$  eV which may be compared with the present experimental value [38]  $\Gamma(\eta \rightarrow \pi^+\pi^-\pi^0)_{\text{expt}} = 267 \pm 25$  eV. The extra effects included involve both the implicitly integrated-out

heavier meson exchanges and partial unitarization to one loop order. One might expect a two loop calculation in the chiral perturbation scheme to be valuable but this may involve too many unknown parameters at the present stage. A dispersion approach using the Gasser-Leutwyler result as a subtraction gave an improved estimate [39]  $\Gamma(\eta \rightarrow \pi^+\pi^-\pi^0) = 209 \pm 20$  eV, which still seems too small.

A possible source of ambiguity arises from the determination of the coefficient of the driving scalar density interaction in Eq.(2). This is determined from the  $K^0 - K^+$  mass difference, which in turn has two components

$$m^2(K^0) - m^2(K^+) = [m^2(K^0) - m^2(K^+)]_{\text{quark mass}} + [m^2(K^0) - m^2(K^+)]_{\gamma}, \quad (3)$$

corresponding to the quark mass differences and the virtual photon emission and reabsorption diagrams respectively. The latter is given in the chiral limit by  $m^2(\pi^0) - m^2(\pi^+)$  according to Dashen's theorem [40] and the reasonable assumption that the photon contribution saturates the pion mass difference. A number of authors [41] have argued that there are important corrections to Dashen's theorem which have the effect of boosting the  $\eta \rightarrow 3\pi$  decay rate.

If one questions Dashen's theorem it is natural to also question Sutherland's result, which deals with the direct electromagnetic contribution to  $\eta \rightarrow 3\pi$ . An investigation of this point yielded [42] the estimate that there was only about a 2% change arising from this, although it decreased rather than raised the rate.

Still another point which may repay further investigation concerns the possible subtleties arising from  $\eta - \eta'$  mixing. An understanding of the  $\eta' \rightarrow 3\pi$  process, for example, might clarify this point. This process has been treated by some authors [43], [44] in the literature but has received only a fraction of the attention given to  $\eta \rightarrow 3\pi$ .

In the present paper we will focus on learning more about the putative nonet of light scalar mesons by studying their contribution to  $\eta \rightarrow 3\pi$ .

### III. CHIRAL SYMMETRY RESULTS TO LOWEST ORDER

For comparison, we first present the well-known results when only the terms present in the lowest order chiral Lagrangian of pseudoscalars are kept.

$$\mathcal{L}_{LO} = \frac{F_\pi^2}{8} \text{Tr}(\partial_\mu U \partial_\mu U^\dagger) + \delta' \text{Tr}[\mathcal{M}(U + U^\dagger)] + \frac{\kappa}{576} \ln^2 \left( \frac{\det U}{\det U^\dagger} \right), \quad (4)$$

where the last term [see Eq.(A14) and comments there] supplies mass to the SU(3) singlet state and  $\mathcal{M}$  is defined in (A11). Fitting  $\mathcal{L}_{LO}$  to the experimental masses determines  $\delta' = F_\pi^2 m_\pi^2 / 8$ .

The  $\eta \rightarrow \pi^+\pi^-\pi^0$  amplitude receives, in this approximation, contributions from diagrams (a), (b) and (c) of Fig.1, which are given in Eq.(B1) (with the non leading corrections deleted). To a reasonable approximation which displays the key dependences these sum up to the lowest order result for the  $\eta \rightarrow \pi^+\pi^-\pi^0$  amplitude

$$M_{0+-}(E_1, E_2, E_3) \approx \frac{16i\delta'y}{F_\pi^4} \cos\theta_p \left(1 - \frac{2E_1}{m_\eta}\right). \quad (5)$$

Here  $E_1$  is the  $\pi^0$  energy in the  $\eta$  restframe and  $y$  is the dimensionless parameter in Eq.(A11) which measures the isospin violation in the quark mass matrix. Assuming Dashen's theorem, Eq.(4) yields

$$8\delta'y = F_\pi^2(m_{K^0}^2 - m_{K^+}^2 - m_{\pi^0}^2 + m_{\pi^+}^2), \quad (6)$$

which allows us to solve for  $y$ . Furthermore  $\theta_p$  is the “nonstrange-strange” pseudoscalar mixing angle defined in Eq.(A15); it is generally taken to be about  $37^\circ$ . It is related to the “octet-singlet” angle,  $\theta$  by

$$\cos\theta_p = \frac{\cos\theta - \sqrt{2}\sin\theta}{\sqrt{3}}. \quad (7)$$

Then Eq.(5) agrees with Eq. (1.14) of [29] except that they neglected  $\eta - \eta'$  mixing by replacing  $\cos\theta_p \rightarrow 1/\sqrt{3}$  in what was denoted the current algebra formula. The matrix element for  $\eta \rightarrow 3\pi^0$  is given in general by

$$M_{000} = M_{0+-}(E_1, E_2, E_3) + M_{0+-}(E_2, E_1, E_3) + M_{0+-}(E_3, E_2, E_1). \quad (8)$$

The widths are then, defining  $\Gamma_{0+-} = \Gamma(\eta \rightarrow \pi^+ \pi^- \pi^0)$  and  $\Gamma_{000} = \Gamma(\eta \rightarrow 3\pi^0)$ :

$$\begin{aligned}\Gamma_{0+-} &= \frac{1}{64\pi^3 m_\eta} \int dE_1 dE_2 |M_{0+-}|^2, \\ \Gamma_{000} &= \frac{1}{384\pi^3 m_\eta} \int dE_1 dE_2 |M_{000}|^2.\end{aligned}\quad (9)$$

Using  $\mathcal{L}_{LO}$ , with parameters determined as described above, we get the tree-level results [from the first terms in each of  $M_{contact}^{a,b,c}$  in Eqs.(B1)]:

$$\begin{aligned}\Gamma_{0+-} &= 106 \text{ eV}, \\ \frac{\Gamma_{000}}{\Gamma_{0+-}} &= 1.40.\end{aligned}\quad (10)$$

These may be compared with the experimental results [38]

$$\begin{aligned}(\Gamma_{0+-})_{\text{expt}} &= 267 \pm 25 \text{ eV}, \\ \left(\frac{\Gamma_{000}}{\Gamma_{0+-}}\right)_{\text{expt}} &= 1.40 \pm 0.01,\end{aligned}\quad (11)$$

which demonstrate the disagreement with experiment for the overall rates in the simplest model. However the width ratio has about the correct magnitude. The related energy spectrum is also about the correct magnitude. The squared matrix element is usually described by quantities  $a$ ,  $b$  and  $c$  defined from

$$|M_{0+-}|^2 \propto (1 + aY + bY^2 + cX^2 \dots), \quad (12)$$

with  $X = \frac{\sqrt{3}}{m_\eta - 3m_\pi}(E_2 - E_3)$  and  $Y = \frac{3}{m_\eta - 3m_\pi}(E_1 - m_\pi) - 1$ . In the present paper we shall not take into account the (not completely negligible) kinematic  $\pi^0 - \pi^+$  mass difference. See [29] for a discussion of this point. The predictions from this simple model,  $a \approx -1$  and  $b \approx 0.25$  are similar to the experimental results [45]  $a_{\text{exp}} = -1.19 \pm 0.07$  and  $b_{\text{exp}} = 0.19 \pm 0.11$  with  $c=0$ .

It is of some interest to also give the predictions for the  $\eta' \rightarrow 3\pi$  decay process at tree level using the simple Lagrangian Eq.(4). It just is necessary (see Appendix B) to replace  $\cos\theta_p$  by  $\sin\theta_p$  and  $m_\eta$  by  $m_{\eta'}$  in Eq.(5) to get for the  $\eta' \rightarrow \pi^0 \pi^+ \pi^-$  matrix element:

$$M'_{0+-}(E_1, E_2, E_3) \approx \frac{16i\delta'y}{F_\pi^4} \sin\theta_p \left(1 - \frac{2E_1}{m_{\eta'}}\right). \quad (13)$$

This leads to the predictions for the  $\eta'$  modes:

$$\begin{aligned}\Gamma'_{0+-} &= 497 \text{ eV}, \\ \Gamma'_{000} &= 562 \text{ eV}.\end{aligned}\quad (14)$$

The experimental results are given as [38]

$$\begin{aligned}(\Gamma'_{0+-})_{\text{exp}} &< 10^4 \text{ eV}, \\ (\Gamma'_{000})_{\text{exp}} &= 315 \pm 56 \text{ eV}.\end{aligned}\quad (15)$$

Only the  $3\pi^0$  mode has really been measured; its width is smaller than predicted in the simple model just presented. One would, of course, expect better agreement for the low energy process  $\eta \rightarrow 3\pi$  for which chiral perturbation theory should be more clearly reliable. In the present paper we shall just make a few remarks on this more complicated process.

It may also be worthwhile to give a rough estimate of the corrections to the rates corresponding to violations of Dashen's Theorem mentioned earlier. If we parameterize the electromagnetic contribution to the  $K^+ - K^0$  mass difference as

$$(m_{K^0}^2 - m_{K^+}^2)_\gamma = f(m_{\pi^0}^2 - m_{\pi^+}^2), \quad (16)$$

where  $f = 1$  corresponds to Dashen's Theorem, we would find by using Eq.(3) that the  $\eta, \eta' \rightarrow 3\pi$  rates predicted for  $\mathcal{L}_{LO}$  should be multiplied by

$$\left[ \frac{(m_{K^0}^2 - m_{K^+}^2) - f(m_{\pi^0}^2 - m_{\pi^+}^2)}{(m_{K^0}^2 - m_{K^+}^2) - (m_{\pi^0}^2 - m_{\pi^+}^2)} \right]^2. \quad (17)$$

For  $f \approx 2$ , which was actually found many years ago [46] the correction factor is about 1.54 and would give  $\Gamma_{0+-} \approx 163$  eV. This corresponds to the overall factor,  $y$  taking the value  $-0.33$  while the Dashen's theorem value used to obtain Eqs.(10) and (14) is  $y = -0.277$ .

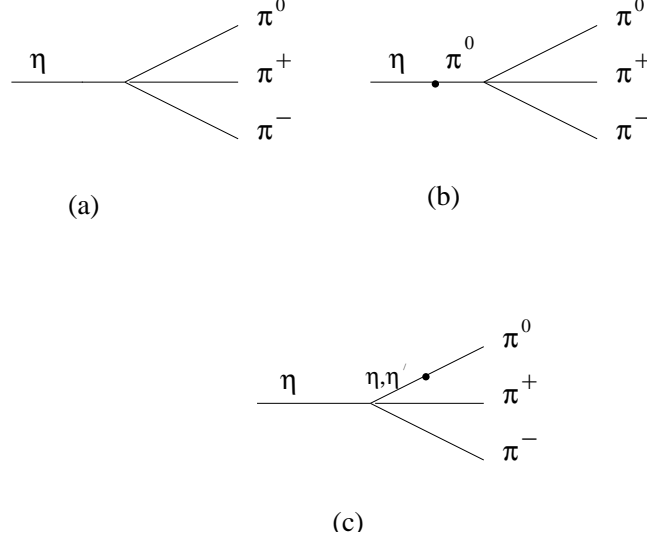


FIG. 1: Feynman diagrams representing the pseudoscalar meson contribution to the decay  $\eta \rightarrow \pi^+ \pi^- \pi^0$ .

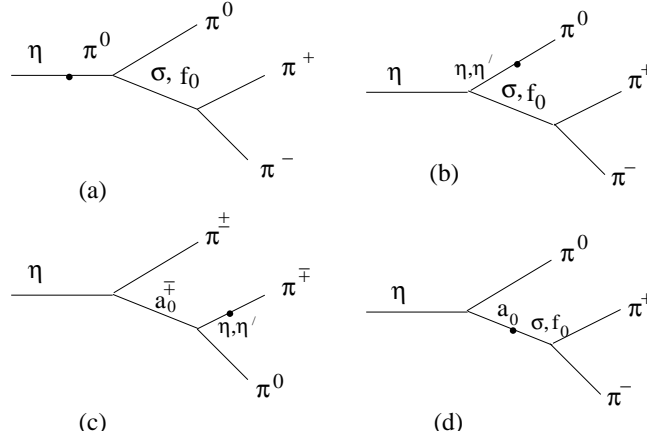


FIG. 2: Feynman diagrams representing the scalar meson contributions to the decay  $\eta \rightarrow \pi^+ \pi^- \pi^0$ .

#### IV. INCLUDING LIGHT SCALAR MESON INTERACTIONS

Now we will study what effects the inclusion of a nonet of light scalar mesons will have on the  $\eta \rightarrow 3\pi$  calculation. We designate the scalar nonet by the  $3 \times 3$  matrix  $N_a^b$  whose interactions are also listed in Appendix A.  $N$  is assumed to contain the well-established  $f_0(980)$  isoscalar and the  $a_0(980)$  isovector as well as the  $\sigma(560)$  and the strange  $\kappa(900)$ . Of these only the  $\kappa(900)$  will not contribute to  $\eta \rightarrow 3\pi$  at tree level. The quark structure of such a nonet has been the subject of much discussion [1]-[28]. If this were an ideal nonet like  $\rho - \omega - K^* - \phi$  one would expect the roughly degenerate  $a_0(980)$  and  $f_0(980)$  to be lowest rather than highest in mass. Actually the masses are better understood intuitively [47] if  $N_a^b$  is an “ideal dual nonet” constructed as  $Q_a \bar{Q}^b$  with  $Q_a \sim \epsilon_{abc} \bar{q}^b q^c$ ;  $q_a$  being the ordinary quark. Then the observed inverted mass ordering is easily seen to follow just from counting the number of strange quarks in  $N_b^a$ . It is important to note that the form of the couplings of  $N_a^b$  to the particles of the non-linear chiral Lagrangian

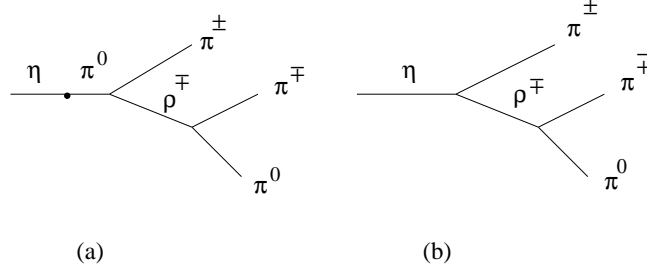


FIG. 3: Feynman diagrams representing the  $\rho$  meson contributions to the decay  $\eta \rightarrow \pi^+ \pi^- \pi^0$ .

being used depend only on the flavor transformation properties of  $N_a^b$ . This does not distinguish different quark substructures. What is sensitive to the quark substructure is the scalar mixing angle,  $\theta_s$ , defined from

$$\begin{pmatrix} \sigma \\ f_0 \end{pmatrix} = \begin{pmatrix} \cos\theta_s & -\sin\theta_s \\ \sin\theta_s & \cos\theta_s \end{pmatrix} \begin{pmatrix} N_3^3 \\ \frac{N_1^1 + N_2^2}{\sqrt{2}} \end{pmatrix}. \quad (18)$$

Small values of  $\theta_s$  would typify a dual ideal nonet while  $|\theta_s|$  about  $\frac{\pi}{2}$  would typify a conventional nonet. Fitting the  $\pi\pi$  and  $\pi K$  scattering amplitudes, including the effects of these scalar resonances, selects [16] the small value  $\theta_s = -20.3^\circ$ .

The scalar nonet mass terms in Appendix A are specified by the four parameters  $(a, b, c, d)$ . The needed chiral invariant scalar -pseudoscalar-pseudoscalar  $S\phi\phi$ -type couplings are specified by the parameters  $(A, B, C, D)$  and the mixing angle  $\theta_s$ . These were all determined from fitting to  $\pi\pi$  scattering,  $\pi K$  scattering and the strong decay  $\eta' \rightarrow \eta\pi\pi$ .

Actually there is reason to believe [48] that the scalars may be best understood as mixtures of a lighter dual nonet and a heavier ordinary nonet. From that point of view, which will be explored more fully in the future, the present single nonet,  $N_b^a$  should be regarded as an approximation to the situation where the heavier (after mixing) particles have been integrated out.

The Feynman diagrams for the scalar contributions to  $\eta \rightarrow \pi^+ \pi^- \pi^0$  are shown in Fig.2. Notice that the diagram in (d) involves new  $a_0 - \sigma$  and  $a_0 - f_0$  isospin violating transitions rather than the  $\pi^0 - \eta$  and  $\pi^0 - \eta'$  transitions which play an important role in the other diagrams. Their strengths  $A_{a\sigma}$  and  $A_{af}$  (see Appendix B) were determined simply by including the effects of isospin violation contained in the spurion matrix  $\mathcal{M}$  in the  $b$  and  $d$  scalar mass terms. Therefore, this does not introduce any new parameters. Actually, the possibility of such contributions was suggested a long time ago [43] as a possible solution of the  $\eta \rightarrow 3\pi$  width problem. Recently a relatively large  $a_0 - f_0$  mixing has been suggested [30] as a way of understanding both anomalously large  $a_0$  central production and the large  $\Gamma(\phi \rightarrow f_0\gamma)/\Gamma(\phi \rightarrow a_0\gamma)$  ratio. However criticisms of this explanation have also been presented [31]. Clearly it may be useful for studies of processes other than  $\eta \rightarrow 3\pi$  to give the coefficients of the scalar isospin violating two point Lagrangian,

$$\mathcal{L} = A_{a\sigma} a_0^0 \sigma + A_{af} a_0^0 f_0, \quad (19)$$

determined consistently with the  $\eta \rightarrow 3\pi$  calculation. Using the parameters from Eq.(A21) in Eq.(B4) we find  $A_{a\sigma} = 0.0170y \text{ GeV}^2$ ,  $A_{af} = 0.0234y \text{ GeV}^2$ , where  $y$  is the quark mass ratio  $\frac{m_u - m_d}{m_u + m_d}$ . Notice that  $y$  (which is negative) is an overall factor for the  $\eta \rightarrow 3\pi$  amplitude in the present model.

We would like to discuss the effects of the scalars when added to the more realistic Lagrangian presented in Appendix A which contains both pseudoscalars and vectors. This Lagrangian contains additional symmetry breaking terms ( $\alpha_p$  and  $\lambda'$ ) to account for the ratio of pseudoscalar decay constants,  $F_K/F_\pi$  being different from unity as well as a number of terms describing the properties of the vector mesons. Of course, the vector mesons play an important role in low energy processes. Since there are many terms it seems useful to add these new features one at a time. Thus in the present section we will consider just the minimal pseudoscalar Lagrangian,  $\mathcal{L}_{LO}$  [Eq.(4)], to be present in addition to the scalars. Furthermore, it is instructive to look at the contributions to the amplitude from different diagrams in order to see how they combine to give the predicted total  $\eta \rightarrow \pi^+ \pi^- \pi^0$  width. In section III we reviewed the leading order calculation of the  $\eta \rightarrow 3\pi$  amplitude which gives the result  $\Gamma(\eta \rightarrow \pi^+ \pi^- \pi^0) = 106 \text{ eV}$  in the Dashen's theorem limit. In Fig.4 we show how the individual contributions of the diagrams in Fig.1 combine to give the leading order amplitude. The magnitude of the  $\eta - \pi^0$  and  $\eta' - \pi^0$  transition coefficients [Eq.(B4) with  $\alpha_p = \lambda' = 0$ , so independent of which state is on-shell] are (in  $\text{GeV}^2$ ):

$$C_{\pi\eta} \approx 0.0042, \quad C_{\pi\eta'} \approx 0.0031. \quad (20)$$

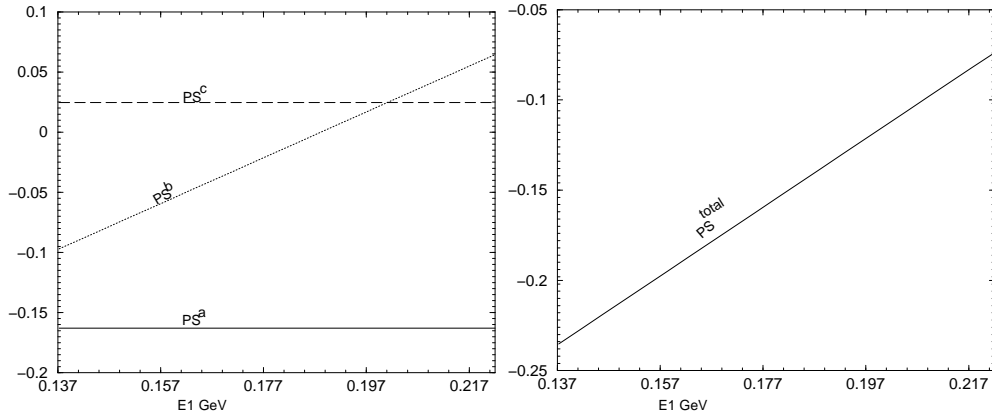


FIG. 4: Plot of different contributions to the leading order  $\eta \rightarrow \pi^+ \pi^- \pi^0$  amplitude as a function of the energy of the neutral pion. On the left, the solid line corresponds to the direct four-point isospin-violating  $\eta \pi^+ \pi^- \pi^0$  vertex of Fig.1a. The energy-dependent dotted line is due to an  $\eta \pi^0$  transition followed by a four-pion contact vertex (Fig.1b). The dashed line is the small contribution due to Fig.1c. (with both  $\eta$  and  $\eta'$  included in the final line). On the right we show the total leading order amplitude, which is the sum of Figs.1a–1c.

Three of the twelve scalar diagrams in Fig.2 can be seen to be larger (by at least an order of magnitude) than all the rest. These are the three diagrams involving the lightest of the scalar mesons,  $\sigma$ , and are contained in Figs.2a, 2b and 2d. For the case of Fig.2b the graph with an  $\eta - \pi^0$  transition dominates that with an  $\eta'$  transition because the latter is suppressed by the (square of) the  $\eta'$  mass in the denominator of the propagator and also the smallness of the associated coupling constants/transition coefficients. In Fig.5 we present the  $\eta \rightarrow \pi^+ \pi^- \pi^0$  amplitudes arising from the three diagrams just mentioned and notice that they cancel almost completely. In particular the  $\sigma$  exchange diagrams in Figs.2a and 2b have opposite signs, as expected – their structure is roughly similar except the propagators have a relative minus sign. We note also that the new isospin violating diagram, involving an  $a_0 - \sigma$  transition, turns out not to lead to dramatically larger contributions than the other diagrams. The cancellation between different diagrams involving the sigma means that the total scalar contribution to the  $\eta \rightarrow \pi^+ \pi^- \pi^0$  width is smaller than might be expected and in fact arises mainly from the  $a_0^\pm$  exchanges in Fig.2c. Comparing Fig.5b with Fig.4b shows that the net scalar contribution does enhance the overall  $\eta \rightarrow \pi^+ \pi^- \pi^0$  rate. Specifically, including the scalar contributions with the pseudoscalar Lagrangian  $\mathcal{L}_\mathcal{O}$  has increased  $\Gamma_{0+-}$  by 16 per cent, from 106 eV to 124 eV. The ratio  $\Gamma_{000}/\Gamma_{0+-}$  is essentially unchanged.

Actually, the calculations above have neglected the finite widths of the  $\sigma$ ,  $f_0$  and  $a_0$  particles. We take these into account by making the replacements in the corresponding propagators [see Eq.(B2)]:

$$\frac{1}{m_X^2 + q^2} \rightarrow \frac{1}{m_X^2 + q^2 - im_X \Gamma_X}, \quad (21)$$

where X stands for  $\sigma$ ,  $f_0$  or  $a_0$ . The  $\Gamma_X$  are given in Appendix A. These replacements modify the result to  $\Gamma_{0+-} = 120$  eV, a 13 per cent increase relative to the leading order result. The width effect is mainly due to the  $\sigma$  propagator.

We may note that the improvement due to the scalars is consistent with the lower values of the prediction,  $160 \pm 50$  eV obtained from the next order of chiral perturbation theory in ref.[29]. The numerical amount of suppression of the scalar contribution to the decay rate from cancellation of Figs. (a) and (b) of Fig.2 is due to the fitted values of  $\gamma_{\sigma\pi\pi}$  and  $\gamma_{\sigma\eta\eta}$  given in Eq.(A22). If we wanted to raise the predicted rate to about 150 eV (still keeping Dashen's theorem in the evaluation of  $y$ ) it would be necessary to raise  $\gamma_{\sigma\eta\eta}$  to about 10.

## V. EFFECTS OF HIGHER ORDER PSEUDOSCALAR SYMMETRY BREAKERS

So far we have worked only with the leading order chiral Lagrangian of pseudoscalars and scalars and obtained (to linear order in  $y = -\frac{m_d - m_u}{m_d + m_u}$ ) isospin-breaking amplitudes proportional to  $\delta'$ ,  $b$  and  $d$  in Eq. (A13) of Appendix A. In order to better fit the properties of the pseudoscalar mesons we consider, as mentioned above, the higher-order symmetry breaking terms in Eq.(A13) with coefficients  $\alpha_p$  and  $\lambda'$ . The numerical values of these parameters are obtained in section 4 of Appendix A, based on an overall fitting of pseudoscalar meson properties.

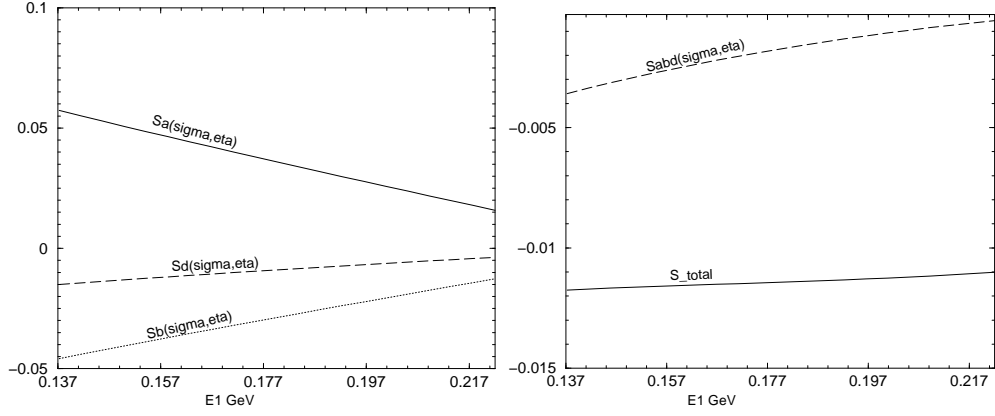


FIG. 5: Scalar meson contributions to the  $\eta \rightarrow \pi^+ \pi^- \pi^0$  amplitude as a function of the energy of the  $\pi^0$ . On the left we show the individually largest contributions – the solid line corresponds to Fig.2a with  $\sigma$  exchange, the dotted line corresponds to Fig.2b with  $\sigma$  exchange and the  $\eta$ - $\pi^0$  transition while the dashed line corresponds to Fig.2d involving the new isospin violating  $a_0 - \sigma$  transition. On the right we show the total amplitude due to the scalar mesons alone. The solid line is due to all of the diagrams in Fig.2 (for the sample value  $E_2 = m_\pi$ ) and the dashed line is the sum of the three largest amplitudes plotted on the left and discussed in the text.

Next we examine the effects of these two new symmetry breaking terms on our previous calculation. It will be seen that these effects include an interesting redistribution of the contributions from the scalar and pseudoscalar diagrams to the total amplitude. First, the contact diagram Fig.1a will receive corrections due to the  $\alpha_p$  and  $\lambda'$  terms [see Eq.(B1)]. This results in some energy dependence since  $\alpha_p$  gives a four-point derivative coupling. More importantly, the  $\eta - \pi^0$  and  $\eta' - \pi^0$  transition coefficients relevant for  $\eta \rightarrow 3\pi$  now depend on which particle is on-shell and are numerically (in  $\text{GeV}^2$ ):

$$\begin{aligned} C_{\pi\eta}^\eta &\approx -0.00583y, & C_{\pi\eta}^\pi &\approx -0.0151y \\ C_{\pi\eta'}^\pi &\approx -0.0113y. \end{aligned} \quad (22)$$

Since  $C_{\pi\eta}^\eta$  is now considerably suppressed in magnitude, the Feynman amplitude for Fig.1b is now suppressed, while  $C_{\pi\eta}^\pi$  and the amplitude for Fig.1c remain about the same. These results, due to only pseudoscalars, are summarized in Fig.6 which may be compared with Fig.4. The net result is that the total  $\eta \rightarrow \pi^+ \pi^- \pi^0$  amplitude (shown in the second of Fig.6) due to pseudoscalar mesons is reduced compared with the leading order result. The pseudoscalars themselves now give  $\Gamma_{0+-} = 81 \text{ eV}$  rather than  $106 \text{ eV}$ , as in section IV.

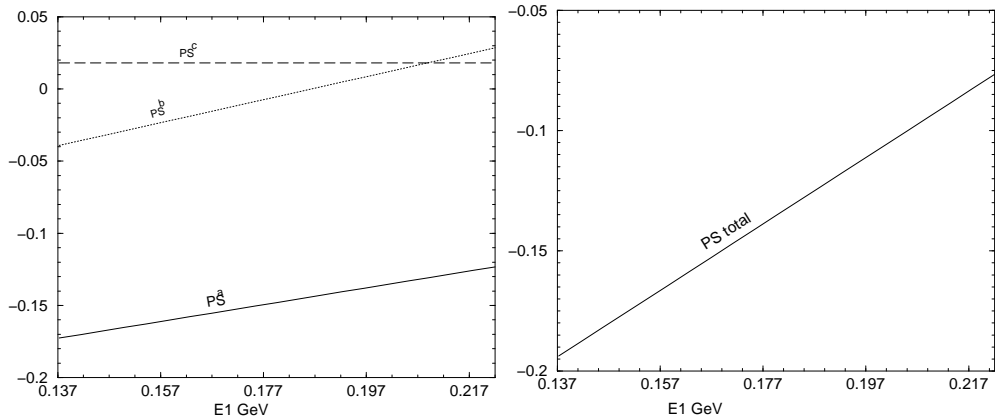


FIG. 6: Left: Contributions due to pseudoscalar mesons alone, taking into account higher order symmetry breaking effects encoded in  $\alpha_p$  and  $\lambda'$ . Compare with the first of Figs.4. Right: Total amplitude due to pseudoscalar mesons alone, taking into account  $\alpha_p$  and  $\lambda'$  terms (compare with second of Figs.4).

However, for the diagrams involving scalar mesons the effect of higher order symmetry breaking is even more important. As we noted above, the scalar meson contribution to  $\eta \rightarrow \pi^+ \pi^- \pi^0$  was rather small as the main diagrams



tended to cancel. When we include the  $\alpha_p$  and  $\lambda'$  corrections to the  $\eta\pi^0$  transition this cancellation will not be so complete. Specifically, comparing Eqs.(20) and (22) we see that the magnitude of the amplitude for Fig.2a, where the  $\eta - \pi^0$  transition occurs with an on-shell  $\eta$ , will be reduced by a factor of approximately four, while that of Fig.2b, where the  $\eta - \pi^0$  transition has an on-shell pion, will remain about the same relative to our result in Section IV. Fig.2d will be unchanged. There will now be a non-negligible contribution from the scalar mesons. It will be more negative in sign (the contribution from Fig.2a is positive, but now smaller in magnitude) and will add “constructively” to the pseudoscalar diagrams in Fig.1 and so increase our prediction for  $\Gamma(\eta \rightarrow \pi^0\pi^+\pi^-)$ . This is shown in Fig. 7. Adding all of the pseudoscalar and scalar diagrams in Fig.1 and Fig.2 with the inclusion of the symmetry breaking effects due to  $\alpha_p$  and  $\lambda'$  we get:  $\Gamma(\eta \rightarrow \pi^0\pi^+\pi^-) = 119.6 \text{ eV}$ . This is essentially the same as the result in section IV but now a larger portion is due to the scalar meson diagrams. Since this is the case the damping effect of the sigma width will be more prominent; in fact it reduces the predicted rate to 103.6 eV in the Dashen’s theorem limit.

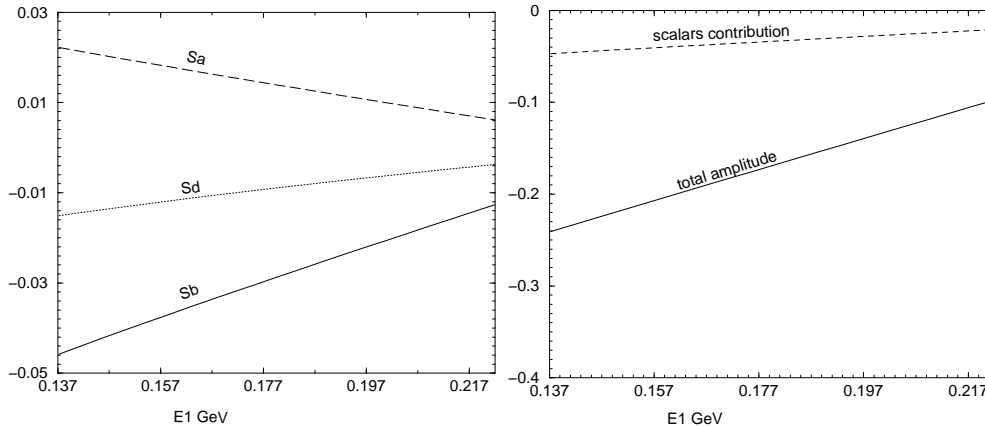


FIG. 7: Left: Contributions due to the three largest scalar meson diagrams, taking into account higher order symmetry breaking effects encoded in  $\alpha_p$  and  $\lambda'$ . Compare with the first of Figs.5. Right: Total amplitude due to pseudoscalar and scalar mesons, taking into account  $\alpha_p$  and  $\lambda'$  terms (compare with second of Figs.6).

It may be of interest to see how the detailed pattern just described depends on the precise value of the quark mass ratio  $x$  and, as explained in section 4 of appendix A, correspondingly on the crucial isospin violating quark mass ratio  $y$ . This is shown for the predicted value of  $\Gamma_{0+-}$  in Table I.

$x, y$	ps. only	ps. + sc. (zero scalar widths)	ps.+sc. (non-zero scalar widths)
20.5, -0.202	63.7 eV	95.9 eV	82.2 eV
23, -0.241	70.7 eV	106.0 eV	91.4 eV
25.1, -0.277	80.2 eV	119.6 eV	103.6 eV

TABLE I:  $\Gamma(\eta \rightarrow \pi^+\pi^-\pi^0)$  for different values of  $x$  and  $y$  defined after Eq.(A11). The second column applies to the case of only pseudoscalars present while the third includes scalars too. The effect of taking non zero scalar widths into account is shown in the last column. Dashen’s theorem is assumed in order to extract  $y$ .

## VI. INCLUDING VECTORS IN THE CALCULATION

It is well known that the inclusion of vector mesons is important for a realistic discussion of low energy chiral dynamics. For example, in the chiral perturbation scheme, most of the finite pieces of the counterterms can be explained by integrating out various vector contributions [49]. In our present approach, of course, we are keeping the resonances, rather than integrating them out, in order to learn more about the scalars.

First, the vector mesons contribute to the  $\eta \rightarrow \pi^+\pi^-\pi^0$  amplitude corresponding to Fig.3a, which is just a correction to  $\pi\pi$  scattering. Its value given by the amplitude,  $M_\rho^a$  in (B3) is easily seen to be comparatively large. However the fourth term of the  $U(3)_L \times U(3)_R$  invariant Lagrangian Eq.(A10) gives, in addition to the  $\rho\pi\pi$  vertex a four pion contact term [included in  $M_{contact}^a$  in (B1)]. Actually this contact term cancels most of the contribution from the

$\rho$ -exchange diagram in Fig.3a. This is well known from chiral treatments of  $\pi\pi$  scattering: when the  $\rho$  is added to the Lagrangian, chiral symmetry requires a contact term which cancels most of the  $\rho$  contribution near threshold, thereby maintaining the current algebra threshold result.

However, the situation is actually a bit more complicated since the process of obtaining an adequate fit to the properties of both the vectors and pseudoscalars [50] requires a number of additional symmetry breaking terms shown in Eq.(A13) of Appendix A. As well as the symmetry breaking terms we have already discussed involving the pseudoscalars alone, there are, in particular, two new terms, measured by the coefficients  $\alpha_+$  and  $\alpha_-$ . It turns out that their effects are very minor. They include an additional contribution to the 4-point isospin violating  $\eta\pi^+\pi^-\pi^0$  vertex due to the  $\alpha_-$  term, corrections to the 4-pion vertex in Fig.1b due to both  $\alpha_+$  and  $\alpha_-$  and an additional diagram, shown in Fig.3b, which contains a new G-parity (and isospin) violating  $\rho\pi\eta$  vertex [the amplitude for this is given as  $M_\rho^b$  in (B3)]. Note that there exists a  $\rho^0 - \omega$  mixing transition, which is the analog of the  $\pi^0 - \eta$  and  $a_0^0 - f_0$  mixing transitions, but it does not contribute to  $\eta \rightarrow 3\pi$  at tree level.

The decay widths with inclusion of vectors are tabulated in Table II for the same values of  $x, y$  used in the last section. In this table the neutral modes are also included. Furthermore, the effect of both the scalar and (actually negligible) vector widths are included too. We see that, as expected from our discussion above, the vectors do not change the overall predictions compared to the last column of Table I very much but they do give a little enhancement. This is also clear by comparing the pseudoscalars + vectors column of table II with the pseudoscalars only column of Table I. It is seen again that the scalars make a non negligible contribution to the total amplitude.

$x, y$	decay mode	ps. +vec.	ps.+sc.+vec.(no width)	ps. +sc. + vec. (width included)
20.5, -0.202	0+-	64.4 eV	96.6 eV	82.8 eV
	000	92.9 eV	139.4 eV	118.9 eV
23, -0.241	0+-	71.9 eV	107.4 eV	92.5 eV
	000	101.9 eV	152.9 eV	131.1 eV
25.1, -0.277	0+-	82 eV	121.7 eV	105.4 eV
	000	114.5 eV	171.3 eV	147.7 eV

TABLE II:  $\Gamma(\eta \rightarrow \pi^0\pi^+\pi^-)$  and  $\Gamma(\eta \rightarrow 3\pi^0)$  for different values of  $x, y$ . In the third column pseudoscalars and vectors are both present. In the fourth and fifth column pseudoscalars, vectors and scalars all present (without and with the effect of the scalar meson widths).

Finally it is interesting to display the energy spectrum parameters  $a, b$  and  $c$  defined in Eq.(12) for the various models we have examined. These are given in Table III and are seen to be reasonable. The  $\chi^2$  measures the fit of our model to the spectrum shape assumed in Eq.(12) and seems to be small.

	$a$	$b$	$c$	$\chi^2$
pseudoscalars(LO)	-1.11	0.31	0	$5.6 \times 10^{-5}$
pseudoscalars	-0.96	0.23	0	$1.5 \times 10^{-4}$
pseudoscalars+scalars	-0.93	0.22	-0.01	$3.3 \times 10^{-4}$
pseudoscalars+scalars+vectors	-1.09	0.26	0.033	$5.8 \times 10^{-3}$

TABLE III: Fits of the energy dependence of the normalized (charged) decay amplitude for  $\eta \rightarrow \pi^0\pi^+\pi^-$  to the form  $|M_{0+-}|^2 = 1 + aY + bY^2 + cX^2$ . The first line corresponds to result at leading order with pseudoscalar mesons only. The second with inclusion of higher order symmetry breakers, the third when scalar mesons are added and the final line when vector mesons are included as well.

## VII. DISCUSSION

We studied the role of a possible nonet of light scalar mesons in the still interesting  $\eta \rightarrow 3\pi$  decay process. Our motivation was primarily to learn more about the scalars themselves. The framework is a conventional non-linear chiral Lagrangian of pseudoscalars and vectors, extended to include scalars (the Lagrangian is described in Appendix A). The parameters involving the scalars were previously obtained to fit the s-wave  $\pi\pi$  and  $\pi K$  scattering in the

region up to about 1 GeV as well as the strong decay  $\eta' \rightarrow \eta\pi\pi$ . An initial concern is whether the model as it stands, containing essentially no undetermined main parameters (up to possible uncertainties in the quark mass ratios  $x = 2m_s/(m_u + m_d)$  and  $y = (m_u - m_d)/(m_u + m_d)$ ), does not make the  $\eta \rightarrow 3\pi$  amplitude too large.

In particular, the  $\sigma(560)$  exchange diagrams (a) and (b) of Fig.2 might lead to a great deal of enhancement due to the possibility of the  $\sigma(560)$ 's momentum being close to mass shell. However this turns out not to be the case. In our initial calculation where the scalars are added to the minimal model of pseudoscalars given in Eq.(4), the left part of Fig.5 shows that these two diagrams, though not individually small, tend to cancel each other. This partial cancellation occurs because the  $\eta - \pi^0$  transition leads to opposite signs when the  $\eta$  is on mass shell and when the  $\pi^0$  is on mass shell (In the first case we have a  $\pi^0$  propagator carrying the momentum squared of an on-shell  $\eta$  while in the second case, the reverse holds). In addition, the enhancement due to the sigma propagator is further suppressed by the inclusion of an imaginary piece, needed to satisfy unitarity in the scattering calculation. The net result is that the effect of including scalars in the minimal pseudoscalar Lagrangian, Eq.(4) is to increase the width for  $\eta \rightarrow \pi^+\pi^-\pi^0$  decay by about 13 per cent. This relatively small, due to cancellation, increase illustrates the difficulty of finding dramatic “smoking gun” evidence for the existence of a light sigma. In the scattering calculation a light sigma appears (see for example [13]) obscured by a large background and does not have a simple Breit Wigner shape.

It is amusing to note the effect of higher derivative terms in the Lagrangian of pseudoscalars (see section V for details). The higher derivative terms allow one to conveniently implement at tree level the fact that the ratio of the pseudoscalar decay constants  $F_{Kp}/F_{\pi p}$  is somewhat greater than unity. With these terms the important  $\pi^0\eta$  transition vertex has a momentum dependent piece. Together with a needed modification in the parameter fitting (see section 4 of Appendix A) this reduces the contribution of the pseudoscalars to the  $\eta \rightarrow 3\pi$  decay width. However the modification of the  $\pi^0 - \eta$  transition noticeably upsets the cancellation between the two sigma exchange diagrams in (a) and (b) of Fig.2. The net result is that, while the total prediction for the  $\eta \rightarrow 3\pi$  decay width remains about the same, now about thirty percent of the value is contributed by the scalars.

The vector meson contribution, discussed in section VI, actually does not change things much. This is because the  $\rho$  exchange diagrams for  $\pi\pi$  s-wave scattering are essentially canceled at very low energies by an extra four pion contact term which automatically arises due to the chiral symmetric formulation. Experimentalists fit the Dalitz plot describing the  $\eta \rightarrow \pi^+\pi^-\pi^0$  spectrum to the form given in Eq.(12). A fit of this type to the predicted spectrum from the Lagrangian of pseudoscalars, scalars and vectors was seen to be close to the experimental one. The basic spectrum shape is already reasonable with the very simplest model discussed in section III. As both the theory and experiment get more precise, the importance of the spectrum shape toward a deeper understanding of the underlying physics increases.

A particularly interesting scalar contribution to  $\eta \rightarrow 3\pi$  arises from the  $a_0 - \sigma$  transition shown in (d) of Fig.2 (The  $a_0 - f_0$  transition contribution to  $\eta \rightarrow 3\pi$  is suppressed due to the propagator of the heavier  $f_0(980)$ ). This is the analog of the important  $\pi^0 - \eta$  transition and, in a sense, is a new mechanism for  $\eta \rightarrow 3\pi$  (although it was investigated a long time ago [43] as a possible way to increase the  $\eta \rightarrow 3\pi$  width). The formula in raw form for this transition is given in Eq.(B4). We evaluated its strength from the knowledge of the isospin violating piece of the dimensionless quark mass matrix  $\mathcal{M}$  in Eq.(A11), determined from the pseudoscalar sector and the coefficients:  $a, b, c$  and  $d$  of the scalar meson mass terms [see Eqs.(A10) and (A13)] determined from the isospin conserving sector of the scalars. However as one can see from the left sides of Figs.5 and 7, the contribution to  $\eta \rightarrow 3\pi$  due to the  $a_0 - \sigma$  transition is not very large, although it has the right sign to boost the decay rate.

The method just described also evaluates the strength of the  $a_0(980) - f_0(980)$  transition. For convenience this is given after Eq.(19), where the overall factor,  $y$  is displayed. This transition has been very much “in the news” recently as a proposed [30] explanation for the large observed  $\Gamma(\phi \rightarrow f_0\gamma)/\Gamma(\phi \rightarrow a_0\gamma)$  ratio and the anomalously strong  $a_0$  central production. However criticisms of this explanation have been given [31], [32], pointing out that the  $a_0 - f_0$  mixing expected from a transition strength like the one determined above is insufficient to give a large effect. Intuitively, because of the near degeneracy of the  $a_0(980)$  and  $f_0(980)$  as well as the similarity of their widths, one might expect the mixing to be very large. But the mixing amplitude is governed by a dimensionless factor  $iA_{af}/(m_a\Gamma_a)$  [see for example Eq.(12) of [32]] which is suppressed by the scalar meson width,  $\Gamma_a$ .

In section II we discussed the current comparison between theory and experiment for the  $\eta \rightarrow \pi^0\pi^+\pi^-$  width. The experimental width [38] is  $\Gamma_{0+-} = 267 \pm 25$  eV. This may be compared with the one loop chiral perturbation theory result [29] of  $160 \pm 50$  eV. More recent attempts [39] to estimate final state interaction effect outside of the chiral perturbation theory approach have increased this somewhat to  $209 \pm 20$  eV. It seems to us that the thirty per cent contribution of the scalars compared to the pseudoscalars we have found should probably not be considered on top of this latter figure. That is because a good portion of the increase due to scalars we have found may be considered as resulting from final state interactions. Many attempts to close the gap between theory and experiment have focused [41] on a reanalysis of electromagnetic corrections to the  $K^+ - K^0$  mass difference. This is argued to increase the quark mass ratio,  $y$  which is an overall factor for the  $\eta \rightarrow 3\pi$  amplitude.

From the standpoint of learning more about the properties of the scalar mesons it is clear that the  $\eta' \rightarrow 3\pi$

decays represent a potentially important source of information. In this case there is sufficient energy available for the  $a_0(980)$  and  $f_0(980)$  propagators to be close enough to their mass shells to avoid suppressing the contributions of these resonances. On the other hand, the theoretical analysis is more difficult since large non-perturbative unitarity corrections are expected. In addition, other more massive particles may also contribute. The experimental information [see Eq.(15)] is more preliminary than in the  $\eta \rightarrow 3\pi$  case. While a number with reasonably small errors has been presented for  $\Gamma'_{000}$ , there is only a weak upper bound for  $\Gamma'_{+-0}$  and also no information on its Dalitz plot. In the model employed in the present paper the  $\eta' \rightarrow 3\pi$  amplitudes are simply obtained from the  $\eta \rightarrow 3\pi$  amplitudes by the simple substitution given in Eq.(B5). Notice that this substitution rule would get modified if a more complicated  $\eta - \eta'$  mixing scheme [e.g. the one mentioned after Eq.(A15)] is adopted. As shown in Eq.(14) the prediction of the minimal model of only pseudoscalars is somewhat too high, but at least of the correct order of magnitude. Adding the scalars without any readjustment of parameters does not improve the prediction for  $\Gamma'_{000}$  but makes it considerably larger (about 2300 eV). A similar large value was recently found in [44]. Since the phase space is fairly large it is perhaps to be expected that large values are typically obtained. Presumably it is a sign for including more detailed unitarity corrections or other physical effects which result in cancellations. We are particularly hopeful that a careful study of mixing between a lower mass exotic scalar nonet and a more conventional higher mass scalar nonet [26, 28, 48] may solve this problem and perhaps contribute to an improved understanding of the  $\eta \rightarrow 3\pi$  decays also.

### Acknowledgments

We are grateful to Masayasu Harada, Paula Herrera-Siklody and Francesco Sannino for very helpful discussions related to this problem. The work of A. A-R. and J.S. has been supported in part by the US DOE under contract DE-FG-02-85ER 40231. D.B. wishes to acknowledge support from the Thomas Jefferson National Accelerator Facility operated by the Southeastern Universities Research Association (SURA) under DOE Contract No. DE-AC05-84ER40150. The work of A.H.F. has been supported by grants from the State of New York/UUP Professional Development Committee, and the 2002 Faculty Grant from the School of Arts and Sciences, SUNY Institute of Technology.

## APPENDIX A: THE CHIRAL LAGRANGIAN

For convenience we collect here needed terms from the pseudoscalar-vector chiral Lagrangian presented in [50] and from the scalar addition presented in [16].

### 1. Transformation Properties

These are constructed to mock up the symmetry properties of the fundamental quark Lagrangian, under which left and right projected light quark fields transform as

$$q_{L,R} \rightarrow U_{L,R} q_{L,R}, \quad (\text{A1})$$

$U_L$  and  $U_R$  being  $3 \times 3$  constant unitary matrices. The pseudoscalar nonet  $\phi(x)$  is a  $3 \times 3$  matrix which fits into the unitary chiral matrix

$$U = \exp\left(\frac{2i\phi(x)}{F_\pi}\right) \quad (\text{A2})$$

where  $F_\pi$  is the (bare) pion decay constant. Under a chiral transformation

$$U \rightarrow U_L U U_R^\dagger. \quad (\text{A3})$$

It is convenient to define the  $3 \times 3$  unitary matrix  $\xi$  by  $U = \xi^2$ . Then  $\xi$  transforms as

$$\xi \rightarrow U_L \xi K^\dagger(\phi, x) = K(\phi, x) \xi U_R^\dagger, \quad (\text{A4})$$

which implicitly defines the unitary matrix  $K$ . The intuitive significance of  $K$  is that the objects  $Kq$  behave like bare quarks surrounded by a pseudoscalar meson cloud, or “constituent quarks”. The objects

$$v_\mu p_\mu = \frac{i}{2}(\xi \partial_\mu \xi^\dagger \pm \xi^\dagger \partial_\mu \xi), \quad (\text{A5})$$

transform as

$$\begin{aligned} p_\mu &\rightarrow K p_\mu K^\dagger \\ v_\mu &\rightarrow K v_\mu K^\dagger + i K \partial_\mu K^\dagger. \end{aligned} \quad (\text{A6})$$

A putative scalar nonet matrix  $N(x)$  is taken to transform as

$$N \rightarrow K N K^\dagger, \quad (\text{A7})$$

The vector meson nonet  $\rho_\mu$  transforms as

$$\rho_\mu \rightarrow K \rho_\mu K^\dagger + \frac{i}{\tilde{g}} K \partial_\mu K^\dagger, \quad (\text{A8})$$

where we have included the dimensionless coupling constant,  $\tilde{g}$ . The “field-strength tensor”

$$F_{\mu\nu}(\rho) = \partial_\mu \rho_\nu - \partial_\nu \rho_\mu - i \tilde{g} [\rho_\mu, \rho_\nu] \rightarrow K F_{\mu\nu} K^\dagger. \quad (\text{A9})$$

## 2. $U(3)_L \times U(3)_R$ Invariant Terms

These comprise the kinetic terms for the three multiplets, mass terms for the scalars and vectors and appropriate interaction terms:

$$\begin{aligned} \mathcal{L}_0 = & -\frac{F_\pi^2}{8} \text{Tr}(\partial_\mu U \partial_\mu U^\dagger) - \frac{1}{4} \text{Tr}(F_{\mu\nu}(\rho) F_{\mu\nu}(\rho)) \\ & - \frac{1}{2} \text{Tr}(\mathcal{D}_\mu N \mathcal{D}_\mu N) - \frac{m_v^2}{2\tilde{g}^2} \text{Tr}[(\tilde{g}\rho_\mu - v_\mu)^2] \\ & - a \text{Tr}(NN) - c \text{Tr}(N) \text{Tr}(N) \\ & + F_\pi^2 \left[ A \epsilon^{abc} \epsilon_{def} N_a^d (p_\mu)_b^e (p_\mu)_c^f + B \text{Tr}(N) \text{Tr}(p_\mu p_\mu) + C \text{Tr}(N p_\mu) \text{Tr}(p_\mu) + D \text{Tr}(N) \text{Tr}(p_\mu) \text{Tr}(p_\mu) \right], \end{aligned} \quad (\text{A10})$$

where  $\mathcal{D}_\mu N = \partial_\mu N - i v_\mu N + i N v_\mu$ . These include the parameters  $m_v^2, a, c, A, B, C$  and  $D$ . Note that the pseudoscalars are still massless at this level. Further note that for the interactions and mass terms of the scalars we do not restrict ourselves to a single trace. For  $q\bar{q}$  mesons the single trace is suggested by the OZI rule while for an ideal dual nonet the  $A$  term is in fact expected to be dominant. We made a fit for  $m_v^2, a, c, A, B, C$  and  $D$  assuming only  $SU(3)$  invariance.

## 3. Symmetry Breaking Terms

The fundamental QCD Lagrangian contains the quark mass term  $-\frac{(m_u+m_d)}{2} \bar{q} \mathcal{M} q$ , with the dimensionless matrix

$$\mathcal{M} = \begin{bmatrix} 1+y & 0 & 0 \\ 0 & 1-y & 0 \\ 0 & 0 & x \end{bmatrix} \quad (\text{A11})$$

where  $x = \frac{2m_s}{m_u+m_d}$  and  $y = -\frac{m_d-m_u}{m_d+m_u}$ .

It is convenient to define

$$\hat{\mathcal{M}}_\pm = \frac{1}{2} (\xi \mathcal{M} \xi \pm \xi^\dagger \mathcal{M} \xi^\dagger). \quad (\text{A12})$$

Then, the symmetry breaking Lagrangian is taken as

$$\begin{aligned} \mathcal{L}_{SB} = & \delta' \text{Tr}[\mathcal{M}(U + U^\dagger)] + \lambda'^2 \text{Tr}[\mathcal{M} U^\dagger \mathcal{M} U^\dagger + \mathcal{M} U \mathcal{M} U] \\ & - \frac{2\alpha_p}{\tilde{g}^2} \text{Tr}(\hat{\mathcal{M}}_+ p_\mu p_\mu) + 2\alpha_+ \text{Tr}\left[\hat{\mathcal{M}}_+ \left(\rho_\mu - \frac{v_\mu}{\tilde{g}}\right) \left(\rho_\mu - \frac{v_\mu}{\tilde{g}}\right)\right] \\ & - \frac{2\alpha_-}{\text{Tr}} \left(\hat{\mathcal{M}}_- \left[\left(\rho_\mu - \frac{v_\mu}{\tilde{g}}\right), p_\mu\right]\right) \\ & + 2\gamma' \text{Tr}[\hat{\mathcal{M}}_+ F_{\mu\nu}(\rho) F_{\mu\nu}(\rho)] \\ & - b \text{Tr}(N N \mathcal{M}) - d \text{Tr}(N) \text{Tr}(N \mathcal{M}). \end{aligned} \quad (\text{A13})$$

Only the parameters  $\delta'$ ,  $\lambda'^2$ ,  $\alpha_p$ ,  $b$  and  $d$  here contribute to the isospin violating vertices of interest in the present paper. The parameter  $\gamma'$  was included in the overall parameter fit obtained in [50] but its small effect on the isospin-conserving vertices will be neglected.

In addition to the quark mass induced symmetry breaking terms there is an important term induced by instanton effects which breaks just the  $U(1)_A$  piece of  $SU(3)_L \times SU(3)_R \times U(1)_V \times U(1)_A$ . It may be summarized as

$$\mathcal{L}_{\eta'} = \frac{\kappa}{576} \ln^2 \left( \frac{\det U}{\det U^\dagger} \right) + \dots \quad (\text{A14})$$

where  $\kappa$  is a constant essentially proportional to the squared mass of the  $\eta'$  meson. The three dots stand for other terms which will be neglected here but are listed in Eq. (2.12) of [51]. Effectively this term gives an important contribution to the  $\eta'$  mass and an  $\eta - \eta'$  mixing angle defined by

$$\begin{pmatrix} \eta \\ \eta' \end{pmatrix} = \begin{pmatrix} \cos\theta_p & -\sin\theta_p \\ \sin\theta_p & \cos\theta_p \end{pmatrix} \begin{pmatrix} (\phi_1^1 + \phi_2^2)/\sqrt{2} \\ \phi_3^3 \end{pmatrix}. \quad (\text{A15})$$

When the extra terms in Eq. A14 are included they will not only give rise to an additional isospin violating transition but will also modify the  $\eta - \eta'$  mixing transformation above to be the non-orthogonal one given in Eq. (4.9) of [51]. We will not include these effects in the present paper, however.

#### 4. Numerical values of parameters used

For the averaged pseudoscalar masses we used,

$$m_\pi = 0.137 \text{ GeV}, \quad m_K = 0.4957 \text{ GeV}. \quad (\text{A16})$$

In section III we gave the fitted parameters for the lowest order Lagrangian containing only pseudoscalars. This also yields the isospin conserving quark mass ratio  $x = 25.1$  (assuming that  $f$ , defined in Eq. (16) is unity). A refitting of these parameters is necessary when the  $\alpha_p/\tilde{g}^2$  and  $\lambda'^2$  symmetry breaking terms are included. This can be conveniently done following the method used in preparing Table III of [50]. There, a value of  $x$  is assumed and the four quantities  $F_\pi$  (unrenormalized pion decay constant),  $\delta'$ ,  $|\lambda'|^2$  and  $\alpha_p/\tilde{g}^2$  are calculated in terms of the four physical quantities  $m_\pi$ ,  $m_K$ ,  $F_{\pi p} = 0.1307 \text{ GeV}$  and  $F_{K p} = 0.1598 \text{ GeV}$ , using:

$$\begin{aligned} \lambda'^2 &= \frac{(1+x)F_{\pi p}^2 m_\pi^2/16 - F_{K p}^2 m_K^2/8}{1-x^2}, \\ \delta' &= F_{\pi p}^2 m_\pi^2/8 - 4\lambda'^2, \\ \frac{\alpha_p}{\tilde{g}^2 F_\pi^2} &= \frac{(F_{K p}/F_{\pi p})^2 - 1}{2(1+x) - 4(F_{K p}/F_{\pi p})^2}, \\ F_\pi &= \frac{F_{\pi p}}{(1 + 4\alpha_p/(\tilde{g}^2 F_\pi^2))^{1/2}}, \\ \frac{\alpha_p}{\tilde{g}^2} &= F_\pi^2 \left( \frac{\alpha_p}{\tilde{g}^2 F_\pi^2} \right). \end{aligned} \quad (\text{A17})$$

In addition, the isospin violating quark mass ratio  $y$  is obtained from

$$(m_{K^0}^2 - m_{K^+}^2) - f(m_{\pi^0}^2 - m_{\pi^+}^2) = (4y/F_{K p}^2)(-2\delta' - 8(1+x)\lambda'^2 + m_K^2 \alpha_p/\tilde{g}^2), \quad (\text{A18})$$

for a particular value of  $f$ . To isolate the effects of the scalars we may choose an  $x$  such that, with the value  $f = 1$  corresponding to Dashen theorem, we recover the value  $y = -0.277$  found in sections III and IV. That gives  $x = 25.1$  and

$$\begin{aligned} F_\pi &= 0.128 \text{ GeV}, & \delta' &= 0.0386 \times 10^{-3} \text{ GeV}^4, \\ \alpha_p/\tilde{g}^2 &= 0.176 \times 10^{-3} \text{ GeV}^2, & |\lambda'| &= 0.643 \times 10^{-3} \text{ GeV}^2. \end{aligned} \quad (\text{A19})$$

The needed dependences on the quark mass ratio  $x$  of the parameters involving vector mesons ( $\gamma'$ ,  $\alpha_+$ ,  $\alpha_-$ ,  $m_v$  and  $\tilde{g}$ ) are given in Table 3 of [50]; the additional point  $x = 25.1$  used in Table II above was treated by interpolation.

The masses and widths of the scalars are taken to be (in MeV)

$$\begin{aligned} m_\sigma = 550, \quad m_\kappa = 897, \quad m_{a_0} = 983.5, \quad m_{f_0} = 980 \\ \Gamma_\sigma = 370, \quad \Gamma_{a_0} = 70.0, \quad \Gamma_{f_0} = 64.6. \end{aligned} \quad (\text{A20})$$

Note that the values of  $\Gamma_\sigma$  and  $\Gamma_\kappa$  are not “Breit-Wigner” widths but are chosen to unitarize the  $\pi\pi$  and  $\pi K$  scattering amplitudes. The masses above fix the parameters (in  $\text{GeV}^2$ ) in (A10) and (A13)

$$a = 0.492, b = -0.00834, c = -0.0160, d = -0.00557 \quad (\text{A21})$$

and the mixing angle  $\theta_s = -20.3^\circ$ . The parameters  $A, B, C, D$  define all the trilinear  $S\phi\phi$  coupling constants according to the formulas given in Appendix C of [16]. The needed coupling constants are (in  $\text{GeV}^{-1}$ )

$$\begin{aligned} \gamma_{\sigma\pi\pi} = 7.27, \gamma_{\sigma\eta\eta} = 3.90, \gamma_{\sigma\eta\eta'} = 1.25, \gamma_{\sigma\eta'\eta'} = -3.82, \\ \gamma_{f\pi\pi} = 1.47, \gamma_{f\eta\eta} = 1.50, \gamma_{f\eta\eta'} = -10.19, \gamma_{f\eta'\eta'} = 1.04, \\ \gamma_{a\pi\eta} = -6.87, \gamma_{a\pi\eta'} = -8.02. \end{aligned} \quad (\text{A22})$$

## APPENDIX B: DECAY AMPLITUDE

The Feynman diagrams representing the  $\eta(p) \rightarrow \pi^0(p_1)\pi^+(p_2)\pi^-(p_3)$  decay are shown in Figs.1-3. The contact diagrams (1a, 1b and 1c) receive contributions from the pseudoscalar and vector part of the Lagrangian

$$\begin{aligned} M_{\text{contact}}^a &= i \frac{16y\delta'\cos\theta_p}{3F_{\pi p}^4} + i \frac{8y\alpha_p\cos\theta_p}{3\tilde{g}^2 F_{\pi p}^4} (-3p_2 \cdot p_3 + p \cdot p_1 + p \cdot p_2 + p \cdot p_3) + i \frac{512y\lambda'^2\cos\theta_p}{3F_{\pi p}^4} \\ M_{\text{contact}}^b &= +i \left( 1 - \frac{3m_v^2}{4\tilde{g}^2 F_{\pi p}^2} \right) \frac{C_{\pi\eta}^\eta}{m_\pi^2 - m_\eta^2} \frac{2}{3F_{\pi p}^2} (-2p_2 \cdot p_3 + p_1 \cdot p_3 - p \cdot p_3 + p_1 \cdot p_2 - p \cdot p_2 + 2p \cdot p_1) \\ &\quad + i \frac{2\alpha_p C_{\pi\eta}^\eta}{\tilde{g}^2 F_{\pi p}^4 ((m_\pi^2 - m_\eta^2))} (-2p \cdot p_1 + 2p_2 \cdot p_3 + p_3 \cdot p - p_3 \cdot p_1 + p_3 \cdot p - p_2 \cdot p_1) \\ &\quad + i \frac{8\alpha_p C_{\pi\eta}^\eta}{3\tilde{g}^2 F_{\pi p}^4 (m_\pi^2 - m_\eta^2)} (5p \cdot p_1 - 5p_2 \cdot p_3 - p \cdot p_3 + p_1 \cdot p_3 - p \cdot p_2 + p_1 \cdot p_2) \\ &\quad + i \frac{256\lambda'^2 C_{\pi\eta}^\eta}{3F_{\pi p}^4 (m_\pi^2 - m_\eta^2)} + i \frac{16\delta' C_{\pi\eta}^\eta}{3F_{\pi p}^4 (m_\pi^2 - m_\eta^2)} \\ M_{\text{contact}}^c &= i \frac{16\delta'}{F_{\pi p}^4} \left( \frac{C_{\pi\eta}^\pi \cos^2\theta_p}{m_\eta^2 - m_\pi^2} + \frac{C_{\pi\eta'}^\pi \sin\theta_p \cos\theta_p}{m_{\eta'}^2 - m_\pi^2} \right) \\ &\quad + i \frac{8\alpha_p}{\tilde{g}^2 F_{\pi p}^4} \left( \frac{C_{\pi\eta}^\pi \cos^2\theta_p}{m_\eta^2 - m_\pi^2} + \frac{C_{\pi\eta'}^\pi \sin\theta_p \cos\theta_p}{m_{\eta'}^2 - m_\pi^2} \right) (p \cdot p_1 - p_2 \cdot p_3 + p \cdot p_3 + p \cdot p_2 - p_1 \cdot p_3 - p_1 \cdot p_2) \\ &\quad + i \frac{256\lambda'^2}{F_{\pi p}^4} \left( \frac{C_{\pi\eta}^\pi \cos^2\theta_p}{m_\eta^2 - m_\pi^2} + \frac{C_{\pi\eta'}^\pi \sin\theta_p \cos\theta_p}{m_{\eta'}^2 - m_\pi^2} \right) \end{aligned} \quad (\text{B1})$$

The scalar contributions (Figs.2a, b, c, and d) are:

$$\begin{aligned} M_{\text{scalar}}^a &= -i \frac{2C_{\pi\eta}^\eta \gamma_{\sigma\pi\pi}^2}{m_\pi^2 - m_\eta^2} \frac{(p \cdot p_1)(p_2 \cdot p_3)}{m_\sigma^2 + (p - p_1)^2} + (\sigma \leftrightarrow f_0) \\ M_{\text{scalar}}^b &= -i\sqrt{2} \left( \frac{2C_{\pi\eta}^\pi \gamma_{\sigma\pi\pi} \gamma_{\sigma\eta\eta}}{m_\eta^2 - m_\pi^2} + \frac{C_{\pi\eta'}^\pi \gamma_{\sigma\pi\pi} \gamma_{\sigma\eta\eta'}}{m_{\eta'}^2 - m_\pi^2} \right) \frac{(p \cdot p_1)(p_2 \cdot p_3)}{m_\sigma^2 + (p - p_1)^2} + (\sigma \leftrightarrow f_0) \\ M_{\text{scalar}}^c &= -i \left( \frac{C_{\pi\eta}^\pi \gamma_{a\pi\eta}^2}{m_\eta^2 - m_\pi^2} + \frac{C_{\pi\eta'}^\pi \gamma_{a\pi\eta} \gamma_{a\pi\eta'}}{m_{\eta'}^2 - m_\pi^2} \right) \frac{(p \cdot p_3)(p_1 \cdot p_2)}{m_{a_0}^2 + (p - p_3)^2} + (p_2 \leftrightarrow p_3) \\ M_{\text{scalar}}^d &= -i\sqrt{2} A_{a\sigma} \gamma_{a\pi\eta} \gamma_{\sigma\pi\pi} \frac{(p \cdot p_1)(p_2 \cdot p_3)}{[m_{a_0}^2 + (p - p_3)^2] [m_\sigma^2 + (p - p_1)^2]} + (\sigma \leftrightarrow f_0) \end{aligned} \quad (\text{B2})$$

The  $\rho$  contributions are:

$$\begin{aligned} M_\rho^a &= i \frac{m_\rho^4 C_{\pi\eta}^\eta}{2\tilde{g}^2 F_{\pi p}^4 (m_\pi^2 - m_\eta^2)} \frac{p \cdot p_1 + p_1 \cdot p_3 - p \cdot p_2 - p_2 \cdot p_3}{m_\rho^2 + (p - p_3)^2} + (p_2 \leftrightarrow p_3) \\ M_\rho^b &= i \frac{4\alpha - y \cos\theta_p g_{\rho\pi\pi}}{\tilde{g} F_{\pi p}^2} \frac{p_2 \cdot (p_3 - p_1)}{m_\rho^2 + (p - p_2)^2} + (p_2 \rightarrow p_3) \end{aligned} \quad (\text{B3})$$

The two point vertices are:

$$\begin{aligned} C_{\pi\eta}^\pi &= -\frac{8y \cos\theta_p \delta'}{F_{\pi p}^2} - \frac{64y \lambda'^2 \cos\theta_p}{F_{\pi p}^2} + \frac{4y \alpha_p \cos\theta_p m_\pi^2}{\tilde{g}^2 F_{\pi p}^2} \\ C_{\pi\eta}^\eta &= -\frac{8y \cos\theta_p \delta'}{F_{\pi p}^2} - \frac{64y \lambda'^2 \cos\theta_p}{F_{\pi p}^2} + \frac{4y \alpha_p \cos\theta_p m_\eta^2}{\tilde{g}^2 F_{\pi p}^2} \\ C_{\pi\eta'}^\pi &= -\frac{8y \sin\theta_p \delta'}{F_{\pi p}^2} - \frac{64y \lambda'^2 \sin\theta_p}{F_{\pi p}^2} + \frac{4y \alpha_p \sin\theta_p m_\pi^2}{\tilde{g}^2 F_{\pi p}^2} \\ C_{\pi\eta'}^\eta &= -\frac{8y \sin\theta_p \delta'}{F_{\pi p}^2} - \frac{64y \lambda'^2 \sin\theta_p}{F_{\pi p}^2} + \frac{4y \alpha_p \sin\theta_p m_{\eta'}^2}{\tilde{g}^2 F_{\pi p}^2} \\ A_{a\sigma} &= 2y (b + d) \sin\theta_s - \sqrt{2}y d \cos\theta_s \\ A_{af} &= -2y (b + d) \cos\theta_s - \sqrt{2}y d \sin\theta_s \end{aligned} \quad (\text{B4})$$

Notice that the superscript on  $C$  indicates which of the two particles involved in the  $\Delta I = 1$  transition is on-shell; this only affects the  $\alpha_p$  term which has derivative coupling.

It is not difficult to verify that the  $\eta' \rightarrow \pi^0 \pi^+ \pi^-$  amplitude may be gotten from the one above by simply making the interchanges

$$\eta \leftrightarrow \eta', \cos\theta_p \leftrightarrow \sin\theta_p, \quad (\text{B5})$$

everywhere in Eqs. (B1)-(B3). This should not be done in Eqs. (B4) since changing, for example,  $C_{\pi\eta}^\pi$  to  $C_{\pi\eta'}^\pi$  accomplishes the desired result automatically.

- 
- [1] See the dedicated conference proceedings, S. Ishida et al “Possible existence of the sigma meson and its implication to hadron physics”, KEK Proceedings 2000-4, Soryushiron Kenkyu 102, No. 5, 2001. Additional points of view are expressed in the proceedings, D. Amelin and A.M. Zaitsev “Hadron Spectroscopy”, Ninth International Conference on Hadron Spectroscopy, Protvino, Russia(2001).
  - [2] E. van Beveren, T.A. Rijken, K. Metzger, C. Dullemond, G. Rupp and J.E. Ribeiro, Z. Phys. **C30**, 615 (1986). E. van Beveren and G. Rupp, hep-ph/9806246, 248. See also J.J. de Swart, P.M.M. Maessen and T.A. Rijken, U.S./Japan Seminar on the YN Interaction, Maui, 1993 [Nijmegen report THEF-NYM 9403].
  - [3] D. Morgan and M.R. Pennington, Phys. Rev. **D48**, 1185 (1993).
  - [4] A.A. Bolokhov, A.N. Manashov, M.V. Polyakov and V.V. Vereshagin, Phys. Rev. **D48**, 3090 (1993). See also V.A. Andrianov and A.N. Manashov, Mod. Phys. Lett. **A8**, 2199 (1993). Extension of this string-like approach to the  $\pi K$  case has been made in V.V. Vereshagin, Phys. Rev. **D55**, 5349 (1997) and very recently in A.V. Vereshagin and V.V. Vereshagin, *ibid.* **59**, 016002 (1999) which is consistent with a light  $\kappa$  state.
  - [5] N.N. Achasov and G.N. Shestakov, Phys. Rev. **D49**, 5779 (1994).
  - [6] R. Kaminski, L. Leśniak and J.P. Maillet, Phys. Rev. **D50**, 3145 (1994).
  - [7] F. Sannino and J. Schechter, Phys. Rev. **D52**, 96 (1995).
  - [8] N.A. Törnqvist, Z. Phys. **C68**, 647 (1995) and references therein. In addition see N.A. Törnqvist and M. Roos, Phys. Rev. Lett. **76**, 1575 (1996), N.A. Törnqvist, hep-ph/9711483 and Phys. Lett. **B426** 105 (1998).
  - [9] R. Delbourgo and M.D. Scadron, Mod. Phys. Lett. **A10**, 251 (1995). See also D. Atkinson, M. Harada and A.I. Sanda, Phys. Rev. **D46**, 3884 (1992).
  - [10] G. Janssen, B.C. Pearce, K. Holinde and J. Speth, Phys. Rev. **D52**, 2690 (1995).
  - [11] M. Svec, Phys. Rev. **D53**, 2343 (1996).
  - [12] S. Ishida, M.Y. Ishida, H. Takahashi, T. Ishida, K. Takamatsu and T. Tsuru, Prog. Theor. Phys. **95**, 745 (1996), S. Ishida, M. Ishida, T. Ishida, K. Takamatsu and T. Tsuru, Prog. Theor. Phys. **98**, 621 (1997). See also M. Ishida and S. Ishida, Talk given at 7th International Conference on Hadron Spectroscopy (Hadron 97), Upton, NY, 25-30 Aug. 1997, hep-ph/9712231.



- [13] M. Harada, F. Sannino and J. Schechter, Phys. Rev. **D54**, 1991 (1996).
- [14] M. Harada, F. Sannino and J. Schechter, Phys. Rev. Lett. **78**, 1603 (1997).
- [15] D. Black, A.H. Fariborz, F. Sannino and J. Schechter, Phys. Rev. **D58**, 054012 (1998).
- [16] D. Black, A.H. Fariborz, F. Sannino and J. Schechter, Phys. Rev. **D59**, 074026 (1999).
- [17] J.A. Oller, E. Oset and J.R. Pelaez, Phys. Rev. Lett. **80**, 3452 (1998). See also K. Igi and K.I. Hikasa, Phys. Rev. **D59**, 034005 (1999).
- [18] A.V. Anisovich and A.V. Sarantsev, Phys. Lett. **B413**, 137 (1997).
- [19] V. Elias, A.H. Fariborz, Fang Shi and T.G. Steele, Nucl. Phys. **A633**, 279 (1998).
- [20] V. Dmitrasinović, Phys. Rev. **C53**, 1383 (1996).
- [21] P. Minkowski and W. Ochs, Eur. Phys. J. **C9**, 283 (1999).
- [22] S. Godfrey and J. Napolitano, hep-ph/9811410.
- [23] L. Burakovsky and T. Goldman, Phys. Rev. **D57** 2879 (1998)
- [24] A. H. Fariborz and J. Schechter, Phys. Rev **D60**, 034002 (1999).
- [25] D. Black, A. H. Fariborz and J. Schechter, Phys. Rev. **D61** 074030 (2000). See also V. Bernard, N. Kaiser and Ulf-G. Meissner, Phys. Rev. **D44**, 3698 (1991), and A. H. Fariborz and J. Schechter, Phys. Rev **D60**, 034002 (1999).
- [26] D. Black, A. H. Fariborz and J. Schechter, Phys. Rev. **D61** 074001 (2000).
- [27] L. Celenza, S-f Gao, B. Huang and C.M. Shakin, Phys. Rev. C 61, 035201 (2000).
- [28] D. Black, A.H. Fariborz, S. Moussa, S. Nasri and J. Schechter, Phys.Rev. **D64**, 014031 (2001).
- [29] J. Gasser and H. Leutwyler, Nucl. Phys. **B250**, (1985) 539. Recent reviews include B. R. Holstein hep-ph/0112150 and J. Bijnens and J.Gasser hep-ph/0202242.
- [30] F.E. Close and A. Kirk, Phys. Lett. **B515** 13 (2001); **489**, 24 (2000). The  $a_0 - f_0$  mixing was earlier studied in N.N. Achasov, S. A. Devyanian and G.N. Shestakov, Phys. Lett.**B88**, 367 (1979).
- [31] N.N. Achasov and A.V. Kiselev; hep-ph/0203042.
- [32] D. Black, M. Harada and J. Schechter, Phys. Rev. Lett.**88** 181603 (2002).
- [33] Y. Hara and Y. Nambu, Phys. Rev. Lett. **16** 875 (1966).
- [34] D.G. Sutherland, Phys. Lett. **23**, 384 (1966).
- [35] S. Bose and A. Zimmerman, Nuvo Cimento, **43** A, 1165(1966).
- [36] Y.T. Chiu, J. Schechter and Y. Ueda, Phys. Rev. **161** (1967), 1612. See also R. Ramachandran, Nuvo Cimento, **47**, 669 (1967).
- [37] J. Schechter and Y. Ueda, Phys. Rev. **D2**, 736,(1970); *ibid* **D3**,176 (1971); *ibid* **D5**, 2846(1972). See also S. Weinberg Phys. Rev. Lett. **27** 1688 (1971).
- [38] K. Hagiwara et al., Phys. Rev. **D66**, 010001 (2002).
- [39] J. Kambor, C. Wiesendanger and D. Wyler, Nucl. Phys. **B465** (1996) 215. See also A. Anisovich and H. Leutwyler, Phys. Lett. **B375**, 335 (1996).
- [40] R. Dashen, Phys. Rev. **183**, 1245 (1969).
- [41] J.F. Donoghue, B.R. Holstein and D. Wyler, Phys. Rev. Lett. **69**, (1992) 3444, J.F. Donoghue, B.R. Holstein and D. Wyler, Phys. Rev. **D47** (1993), 2089, J. Bijnens, Phys. Lett. **B306** (1993), 343.
- [42] R. Baur, J. Kambor and D. Wyler, Nucl. Phys. **B460** (1996) 127.
- [43] J. Schechter and Y. Ueda, Phys. Rev. D **4** (1971) 733, W. Hudnall and J. Schechter, Phys. Rev. **D9** (1974) 2111.
- [44] P. Herrera-Siklody, hep-ph/9902446.
- [45] A. Abele et al, Phys. Lett. **B417**, 197(1998).
- [46] R.H. Socolow, Phys. Rev. **137**, B1221 (1965), J.H. Wojtaszek, R.E. Marshak and Riazuddin, Phys. Rev. **136**, B1053 (1964).
- [47] R.L. Jaffe, Phys. Rev. **D15**, 267 (1977).
- [48] In addition to [26] and [28] above see T. Teshima, I. Kitamura and N. Morisita, arXiv:hep-ph/0105107 and F. Close and N. Tornqvist, arXiv:hep-ph/0204205.
- [49] J.F. Donoghue, C. Ramirez and G. Valencia, Phys.Rev. **D39** , 1947 (1989); G. Ecker, J. Gasser, A. Pich and E. de Rafael, Nucl. Phys. **B321**, 311 (1989); G. Ecker, J. Gasser, H. Leutwyler, A. Pich and E. de Rafael, Phys. Lett. **B233**, 425 (1989).
- [50] M. Harada and J. Schechter, Phys. Rev. **D54**, 3394 (1996)
- [51] J. Schechter, A. Subbaraman and H. Weigel, Phys. Rev. **D48**, 339, (1993).